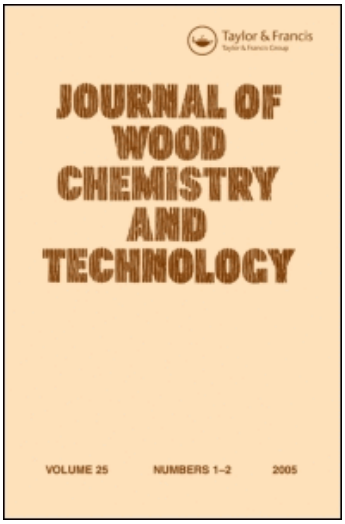

Journal of Wood Chemistry and Technology
Publication details, including instructions for authors and subscription information:
http://www.informaworld.com/smpp/title~content=t713597282

FORMATION AND INVOLVEMENT OF RADICALS IN OXYGEN DELIGNIFICATION STUDIED BY THE AUTOXIDATION OF LIGNIN AND CARBOHYDRATE MODEL COMPOUNDS

Josef Gierer[a]; Torbjörn Reitberger[b]; Erquan Yang[a]; Byung-Ho Yoon[c]
[a] Department of Pulp and Paper Chemistry and Technology—Wood Chemistry, Royal Institute of Technology, Stockholm, Sweden [b] Department of Chemistry—Nuclear Chemistry, Royal Institute of Technology, Stockholm, Sweden [c] Department of Paper Science & Engineering, Kangweon National University, Chunchon, South Korea

Online publication date: 30 November 2001

To cite this Article Gierer, Josef , Reitberger, Torbjörn , Yang, Erquan and Yoon, Byung-Ho(2001) 'FORMATION AND INVOLVEMENT OF RADICALS IN OXYGEN DELIGNIFICATION STUDIED BY THE AUTOXIDATION OF LIGNIN AND CARBOHYDRATE MODEL COMPOUNDS', Journal of Wood Chemistry and Technology, 21: 4, 313 — 341
To link to this Article: DOI: 10.1081/WCT-100108329
URL: http://dx.doi.org/10.1081/WCT-100108329

JOURNAL OF WOOD CHEMISTRY AND TECHNOLOGY, 21(4), 313–341 (2001)

FORMATION AND INVOLVEMENT OF RADICALS IN OXYGEN DELIGNIFICATION STUDIED BY THE AUTOXIDATION OF LIGNIN AND CARBOHYDRATE MODEL COMPOUNDS

Josef Gierer,[1] Torbjörn Reitberger,[2] Erquan Yang,[1] and Byung-Ho Yoon*

Department of Pulp and Paper Chemistry and Technology—Wood Chemistry[1], Department of Chemistry—Nuclear Chemistry,[2] Royal Institute of Technology, Stockholm, Sweden

ABSTRACT

The formation of superoxide and hydroxyl radicals under the conditions of oxygen bleaching and their involvement in the oxidative degradation of lignin and carbohydrate structures have been demonstrated using simple model compounds. It was found that: 1. The first step of autoxidation is a one-electron transfer process yielding a substrate radical and superoxide. Direct coupling between these species in the initial solvent cage is of minor importance. 2. Hydroxyl radicals are formed by a superoxide driven Fenton reaction with a

*Visiting scientist. Present address: Department of Paper Science & Engineering, Kangweon National University, Chunchon, South Korea

pH-maximum in the range 11–11.5. 3. Of the heavy metal salts investigated $CuSO_4$ and $MnSO_4$ facilitate both the degradation of phenolic substrates and the formation of hydroxyl radicals, whereas $FeSO_4$ has no significant effect. 4. Striking mechanistic analogies between the autoxidative degradation of lignin and carbohydrate model compounds determine the *fundamental selectivity* of the process, while formation of hydroxyl radicals determine the *conditional selectivity* imposed on oxygen delignification processes.

INTRODUCTION

Oxygen delignification (bleaching) is a very attractive method to remove lignin from pulp now being implemented in most modern pulp mills. The main advantage of this process is good economy and little environmental impact. However, under current conditions, i.e. high pH and a temperature of ca 100°C, only uncoupled phenolic units and olefinic structures, e.g. of the stilbene and enolether types, are rapidly degraded.[1–3] Coupled phenolic units such as 5-5′-biphenolic structures that originate from protolignin, or arise via radical coupling reactions, are fairly resistant[3] and dominate in residual lignins[4]. In addition, diphenylmethane structures formed during kraft pulping, and non-phenolic β-aryl ether structures are virtually resistant to oxygen treatments. Therefore, lignin elimination would be considerably improved if these resistant structures could be degraded. However, attempts to further delignify the pulp by treatment with oxygen at more rigorous conditions are problematic, due to increased degradation of the polysaccharides, resulting in decrease of pulp strength. Real progress in oxygen delignification presupposes a better understanding of the mechanisms involved. In particular, the role of the reactive intermediates, such as superoxide and hydroxyl radicals, proposed to have a decisive influence on both efficiency and selectivity,[5–7] should be clarified.

In our previous communications,[8–12] superoxide and hydroxyl radicals were generated in a controlled way by γ-radiolytic methods and allowed to react with various types of lignin model compounds. Using this technique, we were able to establish a number of different reaction modes by identifying major reaction products and possible pathways of their formation. The results of these studies can be summarized as follows:

1. *Hydroxyl radicals* readily oxidize phenolic structures to phenoxyl radicals. They also react with non-phenolic substrates by electrophilic addition to aromatic rings forming isomeric hydroxycyclohexadienyl

MARCEL DEKKER, INC.
270 Madison Avenue, New York, New York 10016

radicals or by hydrogen abstraction from aliphatic residues affording carbon-centered radicals. In the presence of oxygen, these radical intermediates are oxidized to hydroxylated-, dealkoxylated- and C_α–C_β cleavage products, as well as to carbonyl-containing structures, with concomitant formation of superoxide. Hydroxyl radicals alone can not degrade aromatic rings into aliphatic structures.

2. *Superoxide* readily reacts with phenoxyl and carbon-centered radicals. The reaction with phenoxyl radicals is characteristic of superoxide and is *not* given by molecular oxygen to any significant extent. This reaction may lead to ring opening or cleavage of a carbon–carbon bond in a ring-conjugated side chain. Reaction products, arising via ring opening, e.g. muconic acid and furane carboxylic acid derivatives, conclusively show the formation of superoxide as intermediate in oxygen degradation of lignin. In the absence of superoxide, phenoxyl, such as guaiacyl, radicals undergo radical coupling, forming biphenolic structures.

In the present work, the results of these radiolysis studies are compared with those obtained when the same model compounds are exposed to autoxidation. The formation of hydroxyl radicals and superoxide under these conditions, and their reactions with model compounds have been studied at different pH-values. Some effects of temperature and transition metal salts have also been investigated.

EXPERIMENTAL

Materials

Creosol, anhydrous $MgSO_4$ and 2,3-dihydro-1,4-phthalazinedione (phthalic hydrazide) were purchased from Aldrich (Germany). *t*-Butyl substituted guaiacol (TBG) was synthesized according to Rosenwald[13] and *t*-butyl-substituted syringol (TBS) according to Adderley, and Hewgill.[14] The non-phenolic model compound 3,4-dimethoxyphenylglycol (''veratrylglycol'', VG) was prepared by bromination of acetoveratrone, followed by acetylation of the resultant bromoacetoveratrone and treatment of the acetate with lithium aluminium hydride.[15] The carbohydrate models glucopyranose and methyl glucopyranoside were obtained from Sigma (USA). $MnSO_4 \times H_2O$, $CuSO_4 \times H_2O$ and $FeSO_4 \times H_2O$ were obtained from Merck (Germany). All these chemicals, as well as the other chemicals used in the experiments and analyses, were of p.a. grade.

The water used as solvent was deionized and filtered through a Milli-Q system (Millipore, USA) or was distilled twice in a quartz apparatus. The

pH of the sample solutions was adjusted with 30% NaOH (Suprapur®, Merck). N_2O-gas, containing less than 10 ppm O_2, was obtained from AGA (Sweden). O_2 (N48) and Ar (N57) were obtained from ALFAX (Sweden).

Treatments with Oxygen

Aqueous sample solutions (100 mL) containing one of the model compounds (1.5 mM) or a mixture of two (0.75 mM of each), phthalic hydrazide (0.6 mM), NaOH (pH adjusted to 11.5–12.4) and, in certain experiments, different metal ions in the concentration range from 0 to 3000 μM, were prepared and transferred to a 250 mL autoclave equipped with a teflon FEP liner. The autoclave was degassed with argon and heated to 90°C in a thermostated water bath. When the sample solution reached the reaction temperature, the autoclave was pressurized with oxygen to obtain a constant pressure of 5 bar and these conditions were maintained for 2 h.

Analyses

During the course of the experiment, sample solutions (2×3 mL) were withdrawn from the reaction mixture through a thin Teflon tubing in the autoclave at chosen intervals and analyzed. After the sample solution had been withdrawn, the autoclave was again pressurized with oxygen to 5 bar and this pressure was maintained during the rest of the experiment.

HPLC-Analyses

The degradation of the lignin model compounds and the formation of reaction products were followed by HPLC analyses, performed on a Pye Unicam HPLC system, equipped with a C-18 reversed-phase column and a diode array UV-detector (PU 4021). Elution gradients of acetonitrile in water (both solvents containing 0.1% acetic acid) were 0–10% (8 min), 10–50% (12 min) and 50–100% (5 min). The elution rate was 2.0-mL/min. The aqueous samples were injected with a WISP 710B autoinjector into a C-18 reverse phase column and directly analyzed by HPLC without prior extraction and derivatisation. Some separations were performed on a 150×4.6-mm column.

The degradation of carbohydrate models was followed by HPLC analyses, run on a Pye Unicam HPLC system, equipped with an ALTEX RI detector and a Waters injector. The elution was performed with water on a thermostated ALTEX C-18 reversed phase column (Ultrasphere TM-ODS 5Ue 967N) at a flow rate of 0.5 mL/min.

GC-MS-Analyses

GC-MS analyses were carried out on a HP 5890 gas chromatograph equipped with a DB-1 column (30 m × 0.32 mm and 0.1 mm film thickness) and interfaced to a Finnigan INOCOS 50 quadrupole instrument (electron impact energy 25 eV). Helium was used as carrier gas (flow rate 10 mL/min). A single temperature ramp program (holding at 80°C for 1 min and then heating to 300°C at a rate of 15°C/min) was used. The injector temperature was 280°C. If necessary, the sample was acetylated, methylated or esterified (using the ion-exchange method) before GC-MS analysis.

Chemiluminescence (CL)-Analyses

The formation of hydroxyl radicals during the autoxidation processes was followed using the chemiluminescence method. This method is based on aromatic hydroxylation of non-chemiluminescent phthalic hydrazide to give 3-hydroxyphthalic hydrazide, which on oxidative degradation produces strongly luminescent 3-hydroxyphthalic acid. Details of the method have been previously described.[16,17]

RESULTS AND DISCUSSION

Autoxidation of Lignin Model Compounds

The driving force of oxygen delignification is the four-electron reduction of molecular oxygen to water:

$$O_2 + 4e^- + 4H^+ \rightarrow 2H_2O$$

This reaction is strongly exothermic and would, if realized, allow oxidation of all lignin components of pulp. However, molecular oxygen is a triplet in the ground state (T_0). Therefore, in the uncatalyzed reduction of oxygen, mechanistic rationale precludes utilization of this energy in a primary

MARCEL DEKKER, INC.
270 Madison Avenue, New York, New York 10016

electron transfer step. Instead, the oxygen reduction proceeds in four consecutive one-electron steps:[18]

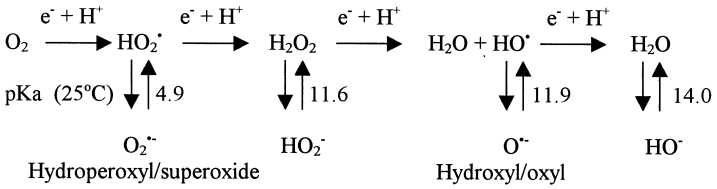

In the uncatalyzed oxygen delignification, the initial step is a one-electron transfer from the substrate (pulp) to oxygen. The standard one-electron reduction potential of O_2 is $-0{,}33$V vs. NHE [19] and is independent of pH above pH 5. Hence, this initial step is not energetically favorable and proceeds at a reasonable rate only with easily oxidized substrates. Oxidation potentials plotted vs. pH for some lignin model compounds[20] are shown in Figure 1.

Evidently, the oxidation potentials of phenolates are significantly lower than those of undissociated phenols and phenol ethers. For this reason, oxygen delignification is usually performed under alkaline conditions and the most probable initial step is an outer-sphere one-electron transfer from phenolate to oxygen. This would result in an initial triplet pair consisting of a phenoxyl radical and superoxide in a solvent cage.[21]

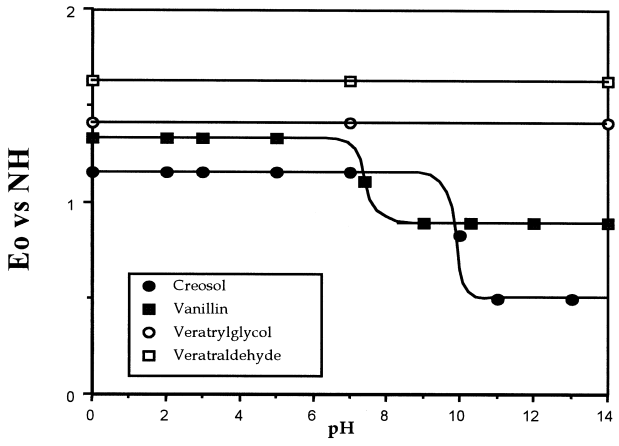

Figure 1. Oxidation potentials for some lignin model compounds plotted vs. pH.

MARCEL DEKKER, INC.
270 Madison Avenue, New York, New York 10016

Significance of an Initial Solvent Cage

The question arises whether spin-inversion may occur before the solvent cage is dissolved. If so, there will be a prompt recombination of superoxide and the phenoxyl radical affording a reaction channel leading directly to ring opening.

It is not feasible to design an experiment, which demonstrates the significance of an initial solvent cage. Therefore, in an alternative approach, we compared the rate of autoxidation at room temperature of 1 mM 4-*t*-butylsyringol (TBS) in the absence and in the presence of 100 mM creosol (CR).

In TBS autoxidation, coupling between phenoxyl radicals ($TBS^{\bullet}$) is blocked by the two *o*-methoxyl groups. Thus, TBS is only eliminated by the reaction between $TBS^{\bullet}$ radicals and superoxide. Assuming steady state conditions, the production and consumption rates of superoxide are equal. In the alkaline solution (pH = 11.6) the dismutation of superoxide can be neglected (*vide infra*), and thus:

$$\frac{d\left[O_2^{\bullet -1}\right]}{dt} = P\left(O_2^{\bullet -1}\right)_0^{TBS} - k^{TBS}[TBS^{\bullet}]\left[O_2^{\bullet -1}\right] = 0 \tag{1}$$

This leads to the following expression for the consumption rate of TBS:

$$R_0^{TBS} = -\frac{d[TBS]}{dt} = \alpha k^{TBS}[TBS^{\bullet}]\left[O_2^{\bullet -1}\right] = \alpha P\left(O_2^{\bullet -1}\right)_0^{TBS} \tag{2}$$

Alpha (α) designates the fraction of superoxide reacting with $TBS^{\bullet}$ by formation of reaction products, i.e. via ring opening. The remainder, $(1-\alpha)$ leads to reformation of TBS and oxygen.

In the presence of CR, a redox equilibrium between the phenoxyl radicals $TBS^{\bullet}$ and $CR^{\bullet}$ and the phenolates TBS^{-} and CR^{-} is established. A theoretical value for the ratio $[CR^{\bullet}]/[TBS^{\bullet}]$ is obtained from the following equations:

$$TBS^{-} \xleftarrow{\rightarrow} TBS^{\bullet} + e^{-}$$
$$CR^{-} \xleftarrow{\rightarrow} CR^{\bullet} + e^{-} \tag{3}$$

$$e_0^{TBS} + 0.059 \log \frac{[TBS^{\bullet}]}{[TBS^{-}]} = e_0^{CR} + 0.059 \log \frac{[CR^{\bullet}]}{[CR^{-}]} \tag{4}$$

Accepting $e_0^{TBS} = 0.47\,V$ and $e_0^{CR} = 0.50\,V$,[22] we obtain:

$$\frac{[TBS^{\bullet}]}{[CR^{\bullet}]} = 3.22\frac{[TBS^{-}]}{[CR^{-}]} \tag{5}$$

MARCEL DEKKER, INC.
270 Madison Avenue, New York, New York 10016

The solution contained 100 mM CR and 1 mM TBS. However, in the experiment the actual pH became 8.9. Based on corresponding pK_a-values,[23] we calculate $[CR^-] = 3.87\,mM$ and $[TBS^-] = 0.10\,mM$. Using these figures we obtain:

$$\frac{[CR^\bullet]}{[TBS^\bullet]} = 12.0 \tag{6}$$

If we assume steady state conditions and neglect the dismutation of superoxide, the following equation should apply:

$$\frac{d\left[O_2^{\bullet -1}\right]}{dt} = P\left(O_2^{\bullet -1}\right)^{TBS} + P\left(O_2^{\bullet -1}\right)^{CR} - k^{TBS}[TBS^\bullet]\left[O_2^{\bullet -1}\right] - k^{CR}[CR^\bullet]\left[O_2^{\bullet -1}\right] = 0 \tag{7}$$

This gives:

$$P\left(O_2^{\bullet -1}\right)^{TBS} + P\left(O_2^{\bullet -1}\right)^{CR} = k^{TBS}[TBS^\bullet]\left[O_2^{\bullet -1}\right]\left(1 + \frac{k^{CR}[CR^\bullet]}{k^{TBS}[TBS^\bullet]}\right) \tag{8}$$

Since $k^{TBS} = 3.0 \times 10^9\,M^{-1}s^{-1}$ and $k^{CR} = 1.4 \times 10^9\,M^{-1}s^{-1}$,[22] we obtain:

$$R^{TBS} = \alpha k^{TBS}[TBS^\bullet]\left[O_2^{\bullet -1}\right] = 0.15\alpha\left(P\left(O_2^{\bullet -1}\right)^{TBS} + P\left(O_2^{\bullet -1}\right)^{CR}\right) \tag{9}$$

Combining the equations for the consumption rate of TBS in the absence and in the presence of CR, we obtain the following expression:

$$\frac{R^{TBS}}{R_0^{TBS}} = \frac{0.15\left(P\left(O_2^{\bullet -1}\right)^{TBS} + P\left(O_2^{\bullet -1}\right)^{CR}\right)}{P\left(O_2^{\bullet -1}\right)_0^{TBS}} \tag{10}$$

The production rates of superoxide by autoxidation of TBS and CR are given by:

$$P\left(O_2^{\bullet -1}\right)^{TBS} = k_{TBS}[TBS^-][O_2] \tag{11}$$

$$P\left(O_2^{\bullet -1}\right)^{CR} = k_{CR}[CR^-][O_2] \tag{12}$$

In the experiment $[O_2]$ was kept constant by O_2 purging. Consequently, the production rates of superoxide are proportional to the actual concentration of $[TBS^-]$ and $[CR^-]$, respectively. Since TBS has only a

MARCEL DEKKER, INC.
270 Madison Avenue, New York, New York 10016

slightly lower oxidation potential than CR, it is reasonable to assume that $k_{CR} \approx k_{TBS}$. i.e.

$$\frac{R^{TBS}}{R_0^{TBS}} = \frac{0.15(0.10 + 3.87)}{1.00} = 0.6 \tag{13}$$

If there is no cage recombination, we may thus expect that the rate of degradation of 1 mM TBS in the presence of 100 mM CR is about 0.6 of the rate in the absence of CR. Figure 2 shows the decay of 1 mM TBS in the absence and presence of 100 mM CR.

From Figure 2 we obtained that in the presence of CR the decomposition rate of TBS is about 0.55 of the decomposition rate in the unperturbed system. Since this ratio does not differ significantly from the calculated one (Eq. (13)), recombination in an initial solvent cage is probably only of minor importance. This suggests that the autoxidation of phenolic substrates in alkaline solution is predominantly of free radical nature.

Effect of Initial pH on the Autoxidation Rate

Figure 3 shows the consumptions (in %) of *tert*-butylguaiacol (TBG) and *tert*-butylsyringol (TBS) after 12 days autoxidation at room temperature as a function of pH.

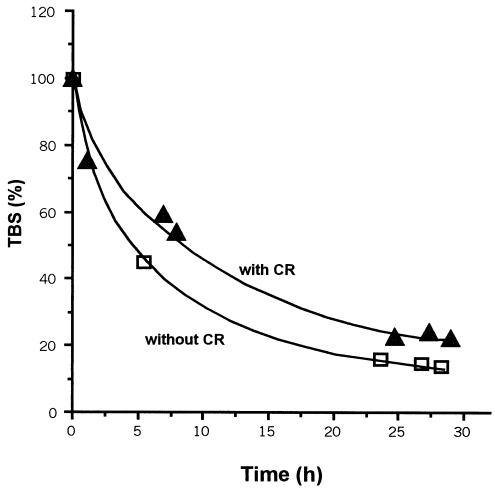

Figure 2. Decomposition of TBS with/without CR present in autoxidation (conditions as described in the text).

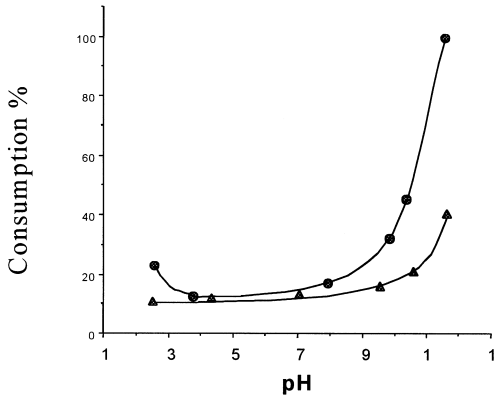

Figure 3. Decay of TBS (●) and TBG (Δ) after 12 days autoxidation at room temperature vs. pH.

As can be seen, the consumptions of both models are very small below the pK_a value (TBG = 10.3 and TBS = 10.0).[23] At pH above the pK_a value the decay dramatically increases, particularly for the syringyl type of model. This strong pH effect reflects the greater ease of phenolates to undergo oxidation, due to their lower oxidation potentials, compared to those of the corresponding (undissociated) phenols. The oxidation potentials of the phenolates from TBS and TBG were found to be 0.47 and 0.53 V, respectively.[22] The difference in the oxidation potentials is ascribed to the additional electron-donating methoxyl group in TBS.

Effect of Temperature on the Autoxidation Rate

The dependence of the rate of consumption of creosol (2 mM) on temperature (20–70°C) was studied at pH 11.6. From the Arrhenius diagram a conditional activation energy of 12.0 kcal/mole (50.1 kJ/mole) was calculated.[24] This value has to be corrected for the decreasing solubility of oxygen with increasing temperature. Using oxygen solubility data,[25] the corrected activation energy becomes 15.4 kcal/mole (64.1 kJ/mole). By combining this activation energy with the decay rate, we estimated the entropy of the reaction to be about 15 e.u. Such a low reaction entropy indicates an outer sphere process, which is in accordance with the presumption that the electron transfer from the creosolate anion to oxygen is the rate-determining

MARCEL DEKKER, INC.
270 Madison Avenue, New York, New York 10016

step. Similar conditional activation energies were obtained in the autoxidation of stilbene[26] and β-aryl ether[2] structures in alkaline medium.

Significance of Superoxide as Intermediate

The preceding discussion suggests that the initial step in autoxidation leads to the generation of $^{\bullet}O_2^-$ by electron transfer from the substrate to oxygen:

$$O_2 + e^- \text{ (from the substrate)} \rightarrow {}^{\bullet}O_2^- \tag{14}$$

Superoxide is the anionic form of the hydroperoxyl radical, $HO_2^{\bullet}$, which is a weak acid with $pK_a \sim 4.8$.[27] Superoxide and the hydroperoxyl radical react at an almost diffusion-controlled rate[27] giving oxygen and hydrogen peroxide:

$$^{\bullet}O_2^- + HO_2^{\bullet} \rightarrow O_2 + HO_2^- \tag{15}$$

In contrast, the rate of the dismutation of two superoxide species is negligible and in practice protons or metal ion species always catalyze this reaction. Above pH 6, the rate of the proton-catalyzed dismutation can be expressed by the equation: $k = 6 \times 10^{(12-\text{pH})}\,M^{-1}s^{-1}$.[27] Thus, under oxygen bleaching conditions, the life-time of superoxide may be considerable. This means that superoxide is diffusible and can penetrate fibres. In organic solvents, superoxide is a strong nucleophile, e.g. it can release Cl^- from CCl_4. In water, however, superoxide is extensively hydrated and its nucleophilic character is much less pronounced.[28] Superoxide acts mainly as a reducing agent, but may also act as a weak oxidant towards molecules with readily transferable hydrogen atoms, e.g. catechols and hydroquinones. In this context, one may consider the following reaction sequence:

$$O_2^{\bullet -} + AOH \rightleftarrows \{HO_2^{\bullet} + AO^-\} \rightarrow HO_2^- + AO^{\bullet} \tag{16}$$

According to this reaction scheme, proton transfer from a phenol to superoxide is directly followed by electron transfer to give the corresponding phenoxyl radical and hydrogen peroxide. Using $pK_a = 4.9$ for $HO_2^{\bullet}$ [27] and pK_a about 10 for lignin-like phenols,[23] the equilibrium constant for the proton transfer is of the order of 10^{-5}. In view of this fact, the suggested reaction may seem unlikely. The electron transfer, however, is energetically favorable since the reduction potential of the hydroperoxyl radical is 0.75 V[29] and the oxidation potential of lignin-related phenolates is about 0.55 V.[22] Given $\lambda^0 = 168\,kJmol^{-1}$,[30] we estimate $k \approx 2 \times 10^5\,M^{-1}s^{-1}$ by the Marcus theory. Hence, the electron transfer may be fast enough to make the overall reaction rate significant. In conventional oxygen delignification,

the direct superoxide driven oxidation of phenols does not play an important part because, under prevailing conditions, phenols are deprotonated and the driving force of the reaction is the formation of the reaction pair depicted within the brackets. In peroxide bleaching, on the other hand, reaction (16) may be important. Experimental support for this view is obtained from column displacement bleaching experiments with unbleached pulp.[31] Unexpectedly, the highest brightness gain was not found at the first but at the second plate. This result implies that hydrogen peroxide at the top level partially decomposes into superoxide which travels down the column with the bleaching liquor and reacts according to the reaction suggested above when pH < 10. Another example of the concomitant abstraction of a proton and an electron by superoxide is the reaction with dihydroxybenzenes affording semiquinone radical anions.[32,33] Although outside the scope of this article, it is interesting to note that reactions of the suggested type were proposed to play a role in the biosynthesis of lignin.[34]

According to radiolysis experiments[10] superoxide is required to bring about cleavage of carbon–carbon bonds (Figure 4). Oxygen and/or hydroxyl radicals cannot directly cause this type of reaction. Thus, the intermediacy of superoxide in autoxidation of lignin is conclusively shown by the

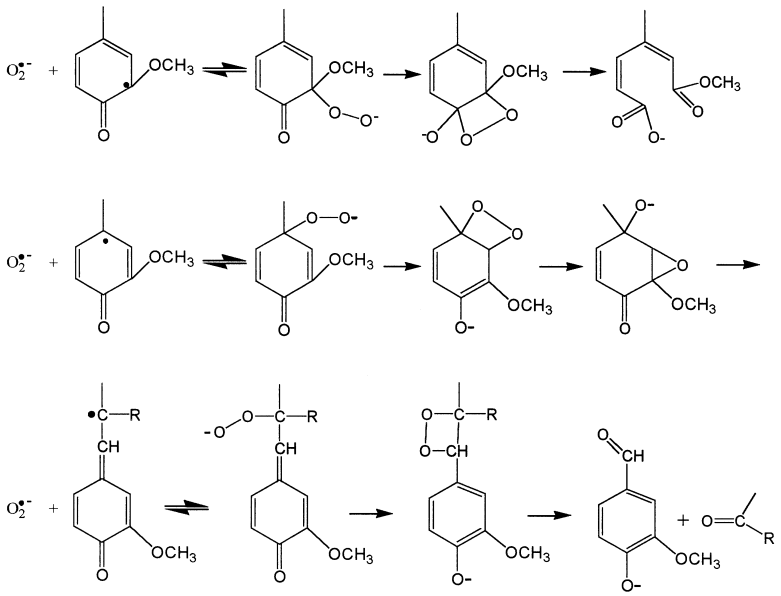

Figure 4. Reaction modes of superoxide.

MARCEL DEKKER, INC.
270 Madison Avenue, New York, New York 10016

formation of products arising from phenoxyl radicals via ring opening, e.g. muconic acid, oxirane and C_α–C_β cleavage products.

Product Pattern vs. pH in Autoxidation of Lignin Model Compounds

In order to study autoxidation under mild conditions, the reactive phenolic model compounds *t*-butylguaiacol (TBG) and *t*-butylsyringol (TBS) were used. Figure 5 shows the product pattern vs. pH after a 12 days autoxidation of TBS and TBG at room temperature.

As expected, the same major products were obtained by autoxidation as by treating the same model compounds with radiolytically generated hydroxyl radicals and superoxide.[10] In the following, only the formation of the major ring opening products, i.e. compounds of the muconic acid ester and furane acid types, will be discussed. During the work-up process, the muconic acid ester type of structure was readily transferred by an acid-catalyzed cyclisation into the corresponding lactone type of structure. The comparison of the yields is more reliable for each product at different pH values than between the different products, since calibration with authentic compounds was not always possible.

In the case of TBS, the formation of muconic acid products increased at the expense of the formation of the *t*-butyl-furane carboxylic acid. These products may therefore arise via a common intermediate, an *ortho*-hydroperoxide (pK_a-value about 11.6). Autoxidation at pH > 11.6

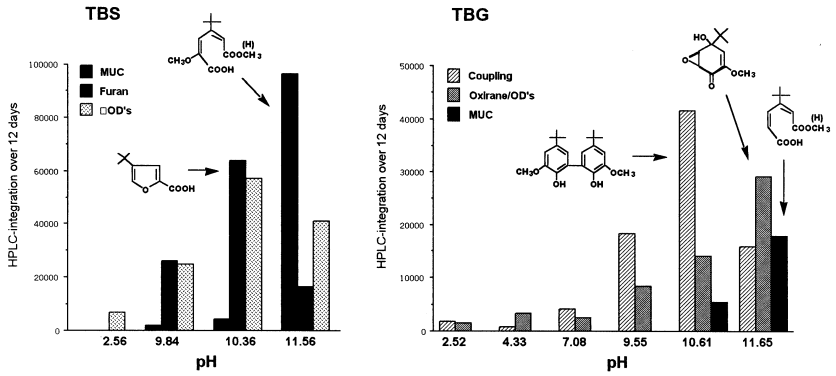

Figure 5. Major reaction products obtained after 12 days autoxidation (room temperature) of TBS and TBG at different pH. OD's refers to the sum of other minor decomposition products.

favors ring opening via the dioxetane mechanism, whereas autoxidation at pH < 11.6 leads predominantly to the formation of the furane carboxylic acid, presumably via hydrolytic cleavage of the hydroperoxide intermediate to give the *ortho*-quinone, and subsequent reaction steps.[35] As expected, no coupling products were detected after autoxidation of TBS.

In the case of TBG, the dominant reaction product at pH < 11 is bis-*t*-butylguaiacol, whereas at higher pH the oxirane and the muconic acid derivative prevail. The latter two products arise via addition of superoxide to the mesomeric forms of the phenoxyl radical from TBG followed by ring closure and rearrangement of the resultant dioxetane. The coupling product bis-*t*-butylguaiacol is formed in competition with the addition of superoxide to the phenoxyl radical. The formation of the coupling product shows an interesting pH-behavior, indicating that there is another reaction consuming superoxide at pH < 11. This may lend support to the suggestion that superoxide can oxidize phenols to the corresponding phenoxyl radicals by a concomitant proton and electron transfer (reaction (16)). Alternatively, the protonated form of the hydroperoxide intermediate may be long-lived enough to hydrolyze and give the *ortho*-quinone, which may subsequently oxidize phenolate to phenoxyl radical.

Significance of the Hydroxyl Radical as Intermediate

It has been repeatedly suggested that the hydroxyl radical, being a very strong oxidant (reduction potential = 2.32 V at pH 7)[36] plays an important role in oxygen delignification.[5,37] It reacts at a diffusion-controlled rate by addition to aromatic nuclei[38] in phenolic as well as in non-phenolic structures and may in this way initiate lignin degradation.[8] However, the hydroxyl radical also attacks carbohydrates by hydrogen atom abstraction at an only marginally lower rate.[36] For this reason, the hydroxyl radical is generally considered to be the main cause of carbohydrate degradation and loss of fiber strength properties. Due to its extreme reactivity the hydroxyl radical is consumed at a site very close to its formation, i.e. only hydroxyl radicals generated in the fiber net work may cause fiber damage.[40]

The hydroxyl radical is a weak acid with a pK_a-value of 11.9 at 25°C.[38] The anionic form, the oxyl radical, O^-, exhibits properties distinctly different from those of the hydroxyl radical. In contrast to the hydroxyl radical, the oxyl radical reacts predominantly by hydrogen atom abstraction.[38] For this reason, the oxyl radical is probably less selective than the hydroxyl radical in its reactions with pulp. The autoxidation and the concomitant formation of hydroxyl radicals were studied using simple phenolic and non-phenolic compounds. When subjected to the conditions of oxygen

MARCEL DEKKER, INC.
270 Madison Avenue, New York, New York 10016

bleaching, creosol (CR) was completely degraded after 90 min (Figure 6, left ordinate). During this degradation the chemiluminescence signal (CL) steadily increased (Figure 6, right ordinate). This shows that the degradation of creosol is accompanied by the formation of hydroxyl radicals, which react with creosol and phthalic hydrazide (PTH) in competition. The continued formation of chemiluminescence after all creosol was consumed can be ascribed to the formation of autoxidable products, in particular bis-creosol.[1]

In contrast, the non-phenolic model 3,4-dimethoxyphenylglycol (''veratrylglycol'', VG) resists this treatment (Figure 7). However, when the phenolic compound (CR) was added before the oxygen treatment of the non-phenolic compound (VG), a significant degradation of the latter took place, giving rise to the formation of veratraldehyde (VA) and 3,4-dimethoxyphenylethanone (''veratrylketone'', VK). As expected, these products were also formed by γ-radiolysis of VG.[15]

These findings conclusively show that during the degradation of CR by oxygen under bleaching conditions hydroxyl radicals are produced and that these radicals bring about partial oxidative degradation of VG which *per se* is resistant towards oxygen under the conditions used.

Hydroxyl radicals may arise directly by a thermally promoted homolytic cleavage of hydroperoxide groups, formed during autoxidation:

$$\text{RO-OH} \rightarrow \text{RO}^{\bullet} + \text{HO}^{\bullet} \qquad (17)$$

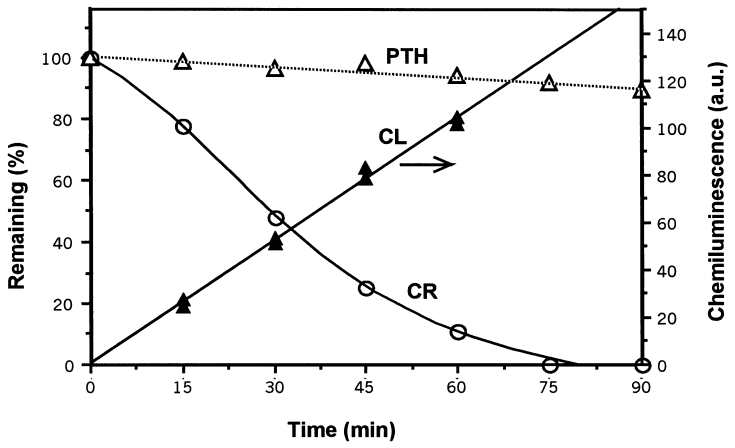

Figure 6. Emission of chemiluminescence (CL) produced by degradation of creosol (CR) in the presence of phthalic hydrazide (PTH) under oxygen bleaching conditions: CR 1.5 mM, PTH 0.6 mM, pH 12.4, O_2 5 bar, 90°C, 120 min.

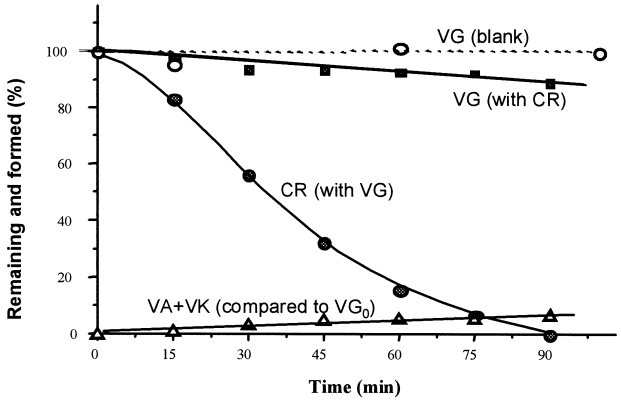

Figure 7. Degradation of veratrylglycol (VG) in the presence of creosol (CR) and formation of VA and VK during the treatment of VG with oxygen under the following conditions: pH 12.4, O_2 5 bar, 90°C, CR 0.75 mM, VG 0.75 mM and VGo 1.50 mM (blank).

Alternatively, hydroxyl radicals may arise indirectly by reductive cleavage of hydrogen peroxide,[38] formed by dismutation of superoxide :

$$H_2O_2 + e^- \rightarrow HO^{\bullet} + HO^- \quad (18)$$

The first alternative, homolytic cleavage of a hydroperoxide intermediate, presupposes the substrate radical $RO^{\bullet}$ be stabilized. In order to obtain experimental support for this reaction mode, the rate of hydroxyl radical formation during autoxidation of *t*-butylguaiacol (TBG) was compared with the corresponding rate during autoxidation of *t*-butyl-syringol (TBS) (Figure 8).

In the case of TBG (left-hand part), the hydroperoxide intermediate, formed by combination of superoxide with the *ortho*-guaiacoxy radical, has two options to react further. The first is intramolecular nucleophilic attack by the peroxy anion, resulting in ring opening with formation of the corresponding muconic acid methyl ester (see Figure 4 upper part). This reaction mode of TBG is common to that of TBS (Figure 8, right-hand part). The second pathway is re-aromatization of the hydroperoxide intermediate to give the corresponding hydroperoxy phenol which can be expected to readily undergo homolytic cleavage of the weak oxygen–oxygen bond, affording a hydroxyl radical and a resonance-stabilized semiquinone radical. On account of this additional source of hydroxyl radicals, TBG should produce these radicals in a larger amount than TBS. However, when the ratios between chemiluminescence formation and phenol degradation were plotted

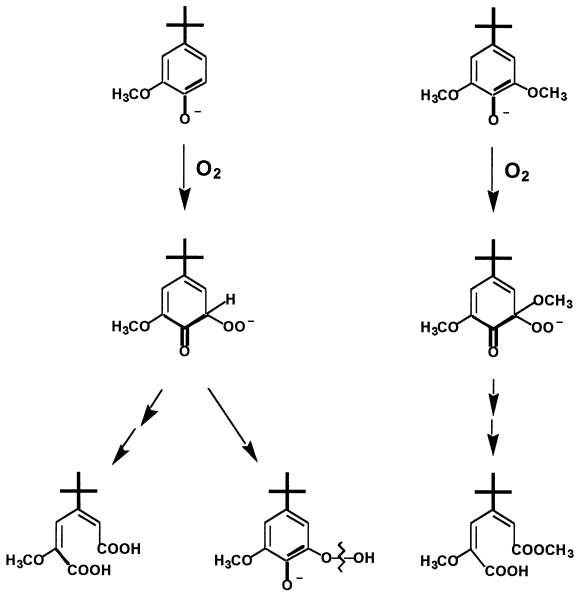

Figure 8. Possible formation of the hydroxyl radical via homolytic cleavage of a hydroperoxide intermediate.

vs. time (Figure 9), practically overlapping curves were obtained, implying that the mode of hydroxyl radical formation during the autoxidation of TBG and TBS is the same.

Thus, the experimental results do not support the supposition that, under the conditions used, hydroxyl radicals arise to any significant extent by homolytic cleavage of hydroperoxides.

The alternative, formation of hydroxyl radicals involves reductive cleavage of hydrogen peroxide (Eq. (18)).[41] In oxygen delignification, this reduction is achieved mainly by superoxide. However, superoxide does not react directly with hydrogen peroxide at any significant rate.[42] In practice this reaction is catalyzed by certain transition metal ions:

$$M^{n+} + O_2^{\bullet -} \rightleftarrows M^{(n-1)+} + O_2 \tag{19}$$

$$M^{n+} + OH^- + HO_2^- \rightleftarrows M^{(n-1)+} + H_2O + O_2^{\bullet -} \tag{20}$$

$$H_2O_2 \rightleftarrows H^+ + HO_2^- \tag{21}$$

$$M^{(n-1)+} + H_2O_2 \rightarrow M^{n+} + OH^- + HO^{\bullet} \tag{22}$$

MARCEL DEKKER, INC.
270 Madison Avenue, New York, New York 10016

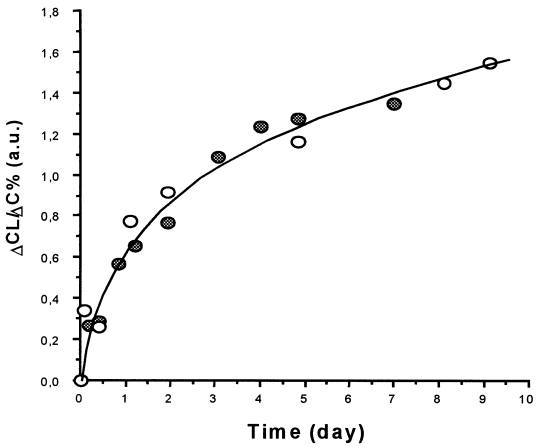

Figure 9. Ratios between chemiluminescence signal and consumption of TBG (●) and TBS (○) as a function of time.

The last step (22) is not an equilibrium reaction, as the hydroxyl radical formed, due to its extreme reactivity,[38] will immediately react with the substrate. According to this mechanism, the rate of formation of hydroxyl radicals (R) can be calculated from the expression:

$$R = q[\mathrm{M}^{n+}][\mathrm{HO}_2^-][\mathrm{H}_2\mathrm{O}_2]^{0.5}[\mathrm{O}_2]^{-0.5} \quad \text{where } q \text{ is a collective constant.} \tag{23}$$

Using this expression, we calculate that the maximum rate of hydroxyl formation lies in the pH range 11–12, i.e. at current conditions of oxygen delignification. It is interesting to note that, in principle at least, the rate of hydroxyl radical formation should be reduced by high oxygen pressure.

The suggested mechanism for the formation of hydroxyl radicals may be regarded as a superoxide-driven Fenton reaction. The cyclic alteration of valence states is governed by the redox potential of the $\mathrm{M}^{(n-1)+}/\mathrm{M}^{n+}$ couple. Redox equilibria are generally proton-dependent. A transition metal may therefore act as a Fenton catalyst only within a certain pH-range. Under alkaline conditions, Mn and Cu catalyze the decomposition of hydrogen peroxide, whereas Fe is inactive. Conversely, Fe is an efficient catalyst in acidic solution, whereas Mn is inactive in this case.[43,44]

Figure 10 shows the extent of creosol degradation and the formation rate of hydroxyl radicals under oxygen bleaching conditions (5 bar oxygen, 90°C) at 5 pH values between pH 10.0 and 12.0.

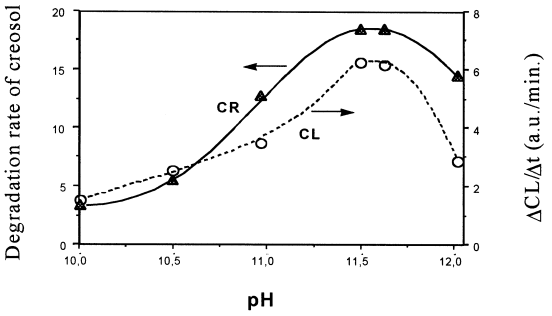

Figure 10. The rate of degradation of CR by oxygen and the formation rate of hydroxyl radicals at 5 pH values between pH 10.0 and 12.0. (3 μM $MnSO_4$ was added to mimic bleaching conditions).

Evidently, the observed pH maximum is in agreement with that calculated on the basis of the superoxide-driven Fenton reaction scheme.

Calibration of the CL-signal in Figure 6 against γ-irradiation of an identical reaction system made it possible to assess the hydroxyl radical production rate associated with autoxidation of CR. This analysis indicates that the initial hydroxyl radical production rate was about $10\,\mu mol\,L^{-1}\,min^{-1}$. Combining this assessment with the initial consumption rate of CR, gives an initial hydroxyl radical yield of about 25%. An analysis of the degradation of VG in Figure 7 was also performed. Assuming that the hydroxyl radical reacts with CR and VG at equal (diffusion controlled) rate, the degradation of VG in relation to that of CR is in accordance with a hydroxyl radical yield of about 25%. Evidently, these assessments of the hydroxyl radical yield indicate in both cases a surprisingly efficient formation of hydroxyl radicals under prevailing conditions. In fact, if the superoxide-driven Fenton reaction were the only source of hydroxyl radicals, the maximum hydroxyl radical yield would be 25%. A possible explanation of this result is that the equilibria in Figure 4 are strongly shifted to the left due to thermal instability of the hydroperoxide anion intermediate.

Autoxidation of Carbohydrate Model Compounds

The reducing sugar glucose was partly degraded by oxygen under bleaching conditions. As is true for creosol, this degradation is accompanied by the formation of hydroxyl radicals. In Figure 11, these two variables are plotted vs. time. In contrast to creosol, the formation of hydroxyl

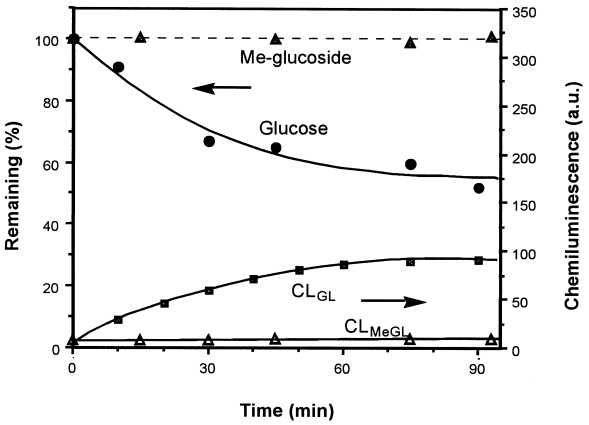

Figure 11. The degradation of glucose and the formation of hydroxyl radicals plotted vs. time.

radicals during autoxidation of glucose appears to be directly coupled to the degradation of the substrate. The reaction is limited to about 50% conversion under prevailing conditions. Similarly, the formation of hydroxyl radicals, as measured by chemiluminescence, ceases at about the same extent of conversion. A possible explanation for this behavior could be a reduction in pH by the acids formed during the oxidative degradation of glucose, which should result in a lower rate of the initial reaction of glucose with oxygen.

Contrary to the behaviour of glucose, the non-reducing derivative, methyl glucoside is stable when treated under similar conditions and does not afford any detectable amount of hydroxyl radicals. However, when the treatment of the methyl glucoside was performed in the presence creosol, an appreciable degradation of the non-reducing sugar model was observed.[42] This result corroborates that during the autoxidation of creosol hydroxyl radicals are generated which bring about the partial degradation of substrates stable towards oxygen, here methyl glucoside. It appears likely that the degradation of non-reducing sugars under oxygen bleaching conditions can also be initiated by reducing sugars.

Comparison Between the Autoxidation of Lignin and Carbohydrate Structures

The initial steps of the autoxidation of creosol and glucose may be formulated as shown in Figure 12. In alkaline solution, creosol and glucose

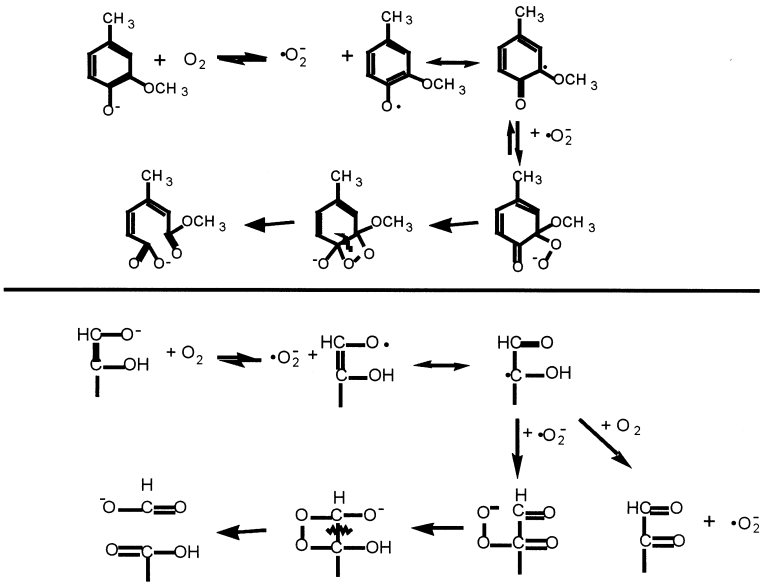

Figure 12. Comparison of the initial steps in the autoxidation of a phenolic group in lignins and a reducing end group in carbohydrates.

are present in their phenolate and enolate forms, respectively, which are oxidized via a one-electron transfer to molecular oxygen, affording the corresponding substrate radical and superoxide. The subsequent reaction step, i.e. addition of superoxide followed by cleavage of a carbon–carbon bond, is also common to both autoxidations and proceeds as already described for creosol. However, in contrast to phenoxyl radicals carbohydrate-derived radicals react also rapidly with oxygen to give carbonyl structures (glucosones) and further oxidation products.[46] The formation of carbonyl structures in cellulose may lead to alkali-induced cleavage of glucosidic bonds (''peeling''). Hence, hydroxyl radicals may cause both direct[47] and indirect cleavage of glucosidic linkages in cellulose.

Selectivity

In view of the striking analogies in the mechanisms of lignin and carbohydrate autoxidation reactions (Figure 12), it is not surprising that the selectivity of oxygen bleaching of pulps is limited. The following

Marcel Dekker, Inc.
270 Madison Avenue, New York, New York 10016

differences and their dependence on the reaction conditions employed, in particular pH and temperature, may determine the degree of selectivity:

1. Different dissociation constants of phenolic and enolic hydroxyl groups.
2. Different oxidation potentials of the phenolate ion/phenoxyl radical and enolate ion/enoxyl radical couples.
3. Different reaction rates when hydroxyl radicals attack lignin and carbohydrates. In particular, the electrophilic addition of hydroxyl radicals to aromatic rings in lignins proceeds 5–6 times faster than the abstraction of hydrogen from carbohydrate structures. These reaction rates were measured directly by pulse radiolysis of aqueous solutions, containing lignin and/or carbohydrate model compound(s).[39] However, γ-radiolysis of aqueous solutions, containing both a non-phenolic lignin and a carbohydrate model compound, showed that the rate of degradation of the lignin model was only twice that of the carbohydrate model.[39] This means that the ''initial selectivity'' does not reflect the ''overall selectivity'' which depends not only on the reaction rates of the hydroxyl radical but also on the reaction modes and rates of the resultant substrate radicals.[47] Thus, the different redox properties of lignin and carbohydrate radicals lead to a more extensive reformation of the lignin model compound as compared to the carbohydrate model, which lowers the ''over all selectivity''. The selectivity may be further decreased by the fact that carbohydrate-derived radicals react with oxygen under the conditions of oxygen bleaching, whereas phenoxyl radicals do not (Figure 12).
4. Different extent of $O_2^{\bullet -}$ reactions with phenoxyl radicals in lignins which undergo C–C cleavage reactions (ring opening, oxirane formation and C_α–C_β scission, Figure 4) and with carbon-centered radicals in carbohydrates which in addition afford carbonyl structures (Figure 12).
5. Different reaction modes of the undissociated and dissociated forms of hydroxyl and hydroperoxyl radicals.

The decreasing selectivity of oxygen bleaching with increasing pH, observed by Yokoyama et al.[47] can easily be explained by an increasing dissociation of $HO^\bullet$ radicals to give $O^{\bullet -}$ radicals which, in contrast to $^\bullet OH$, do not react preferentially by electrophilic addition to aromatic nuclei in lignins.

Effects of Metal Ions on Autoxidation

Considering the fact that all steps in the autoxidation entail redox reactions, it can be expected that these steps will be strongly influenced by

Marcel Dekker, Inc.
270 Madison Avenue, New York, New York 10016

the presence of other redox systems, such as transition metal ion species. These may be involved in four consecutive steps of autoxidation processes, namely in:

1. The initial transfer of an electron from an (activated) substrate molecule to oxygen with formation of superoxide.[48,49]
2. The dismutation of superoxide to give hydrogen peroxide and oxygen.
3. The reductive cleavage of hydrogen peroxide by superoxide to give hydroxyl radicals.
4. The transformation of substrate radicals into reaction products.

The influence of metal ion species was investigated in two different ways. First, we determined how reducing the amount of metal ions present in NaOH affects the rates of creosol consumption and hydroxyl radical formation. According to this approach, the influence of metal ions was reduced by the use of Suprapur® NaOH and by the addition of a complexing agent (0.1 mM DTPA). Apparently, a reduction of the transition metal ion content affects the rate of consumption of creosol (Figure 13) much less than the rate of formation of hydroxyl radicals (Figure 14). The almost complete elimination of the hydroxyl radical formation when metal ion species were excluded is a strong support to the supposition that the superoxide-driven Fenton reaction is the predominant mode of hydroxyl radical formation in autoxidation processes.

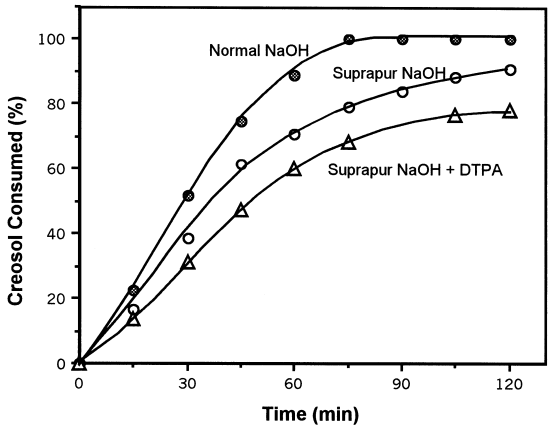

Figure 13. Consumption of creosol during autoxidation in different qualities of NaOH.

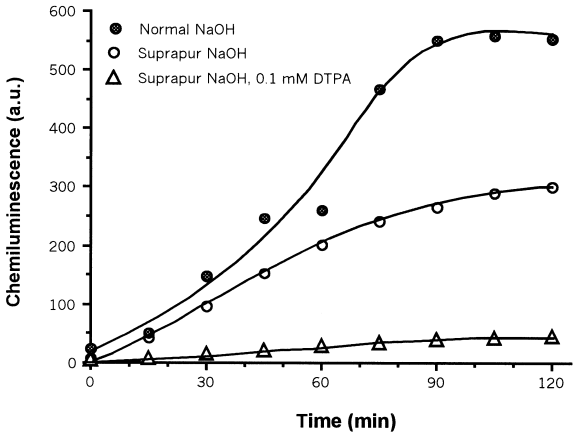

Figure 14. Emission of chemiluminescence during autoxidation of creosol in different qualities of NaOH.

In a second set of experiments, we added known amounts of transition metals ($CuSO_4$, $MnSO_4$ or $FeSO_4$) to solutions containing creosol and Suprapur® NaOH. The rate of substrate degradation and hydroxyl radical formation were followed. It was found that addition of $CuSO_4$ brings about the largest increase in both rates whereas addition of $FeSO_4$ is virtually without effect. As in the previous approach, the differences between the rates of hydroxyl radical formation were much greater than those between the corresponding consumption rates (cf. Figures 13 and 14). In Figure 15, the rates of creosol degradation and hydroxyl radical formation under oxygen bleaching conditions are plotted vs. the concentrations of $MnSO_4$ and $CuSO_4$.

From the shape of the curves in Figure 15, it may be concluded that $CuSO_4$ and $MnSO_4$ affect both these rates in a similar manner. Addition of each of these salts to a concentration of about 3 μM gives a maximal enhancement of the rate of creosol degradation and hydroxyl radical formation. Evidently, the rates are most enhanced when the transition metals are present in trace amounts. This may be interpreted in the following terms:

The formation of hydroxyl radicals via one-electron reduction of hydrogen peroxide in alkaline solution is catalyzed primarily by free mononuclear transition metal ion species. In alkaline solution, such species may only arise when transition metal ions are present in very low concentrations. Accordingly, hydroxyl radical formation by reductive cleavage of hydrogen peroxide is most extensive when traces of transition metals are present. In

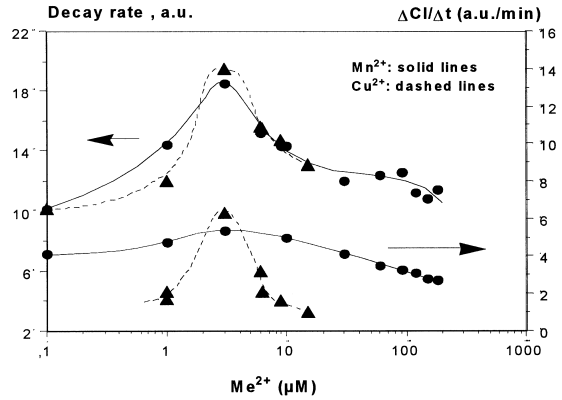

Figure 15. Rates of creosol degradation and hydroxyl radical formation plotted vs. the concentrations of $MnSO_4$ and $CuSO_4$.

higher concentrations, most metal ions aggregate or condense in alkaline solution to form hydroxo-bridged polynuclear species.[50] For example, at pH > 9, Mn^{++} and HO^- ions form aggregates which can be oxidized by molecular oxygen to give MnO_2. Colloidal MnO_2 decomposes hydrogen peroxide efficiently by a two-electron reduction to give oxygen and water directly, i.e. without generating any significant amount of hydroxyl radicals. As a consequence, the rate of hydroxyl radical formation, and, to a minor extent, that of creosol degradation is reduced. Colloidal particles of metal hydroxides and hydrated oxides may not only catalyze the decomposition of hydrogen peroxide, i.e. mimic catalase, but may also catalyze the dismutation of superoxide, i.e. mimic dismutase. In this context, one may consider the possibility that colloidal particles of $Mg(OH)_2$ control the superoxide activity under oxygen bleaching. This could be an additional explanation for the beneficial effect of Mg salts in oxygen bleaching.

In Figure 16, the participation of transition metal ion species in the four steps of oxygen reduction is summerized.

In oxygen and peroxide bleaching of pulp it is common practice to add chelators, such as EDTA or DTPA to improve the viscosity. The effect of these chelators may be explained by the fact that metal ions in a higher valence state are more strongly complexed than ions in lower valence states. As a result, the reduction of chelated metal ions by superoxide to a lower valence state and, thus, the superoxide-driven Fenton reaction are inhibited. One should note, however, that metal ions in the bleaching liquor might affect the viscosity drop only to a small extent. In contrast, metal ions bound

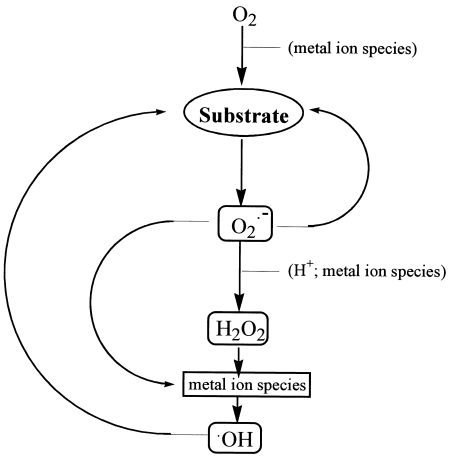

Figure 16. Redox reactions involved in autoxidation catalyzed by transition metal ion species. Only the superoxide driven Fenton reaction requires transition metal ion species. In other redox steps the presence of metal ion species is not conditional.

to the fibers may cause a sustained attack leading to fibre fracture. Evidently, control of transition metals in the fibers is required to reach a good bleaching result. Unfortunately, little is known about how transition metals are bound to the fibers.

CONCLUSIONS

The results of the present work may be summarized as follows:

1. Autoxidation and γ-irradiation of lignin models give the same product pattern. This implies similar reaction steps in both treatments involving superoxide and hydroxyl radicals as intermediary oxidants.
2. The first step of autoxidation is a one-electron transfer process yielding a substrate radical and superoxide. Direct coupling between these species in the initial solvent cage is insignificant.
3. Superoxide plays a central part in autoxidative processes:
   a) as the reagent required for the opening of aromatic rings and for the cleavage of other carbon–carbon linkages in lignins,
   b) as source of hydroxyl radicals which attack both lignins and carbohydrates,

c) as a weak oxidant towards molecules with readily transferable hydrogen atoms, e.g. phenols.

4. Hydroxyl radicals are generated under oxygen bleaching conditions within the pH range 10–12 mainly in a superoxide-driven Fenton reaction. Formation of hydroxyl radicals via homolytic cleavage of hydroperoxy intermediates appears to be insignificant. Of the metals investigated, Cu and Mn facilitate both the degradation of phenolic substrates and the formation of hydroxyl radicals, whereas Fe has no significant effect.

5. Striking mechanistic analogies between the autoxidative degradation of lignin and carbohydrate model compounds determine the *fundamental selectivity* of the process, while 3a and 3b explain the *conditional selectivity* restrictions imposed on oxygen delignification processes.

REFERENCES

1. Ljunggren, S. Nordic Pulp & Paper Res. J. **1990**, *5*, 38.
2. Ljunggren, S.; Johansson, E. Holzforschung **1990**, *44*, 29.
3. Ljunggren S.; Johansson, E. Nordic Pulp & Paper Res. J. **1990**, *5*, 148.
4. Gellerstedt, G.; Gustafsson, K.; Lindfors, E.-L. Nordic Pulp & Paper Res. J. **1986**, *1*, 14.
5. Gierer, J. Holzforschung **1990**, *44* (5), 387, *44* (6), 395.
6. Brolin, A.; Gierer, J.; Zhang, och Y. Wood Sci. Technol. **1993**, *27*, 115.
7. Eriksson, T.; Gierer, J. *Proc. Int. Symp. Wood and Pulping Chem.*, Raleigh, N.C. USA, 1989; Vol. 2, 59–63.
8. Gierer, J.; Yang, E.; Reitberger, T. Holzforschung **1992**, *46*, 495.
9. Gierer, J.; Jansbo, K.; Reitberger, T. J. Wood Chem. Technol. **1993**, *13*, 561.
10. Gierer, J.; Yang, E.; Reitberger, T. Holzforschung **1994**, *48*, 405.
11. Gierer, J.; Yang, E.; Reitberger, T. Holzforschung **1996**, *50*, 342.
12. Gierer, J.; Yang, E.; Reitberger, T. Holzforschung **1996**, *50*, 353.
13. Rosenwald, R.H. J. Am. Chem. Soc. **1952**, *74*, 4602.
14. Adderley, C.J.K.; Hewgill, F.R. J. Chem. Soc. **1968**, *C*, 1438.
15. Jansbo, K. *Diss. Royal Inst. of Techn.*, Dept. of Wood Chemistry, 1993.
16. Reitberger, T.; Gierer, J. Holzforschung **1988**, *42*, 351.
17. Backa, S.; Jansbo, K.; Reitberger, T. Holzforschung **1997**, *51*, 557.
18. Sawyer, D.T.; Nanni, E.J., Jr. In *Oxygen and Oxy-radicals in Chemistry and Biology*. Rodgers, M.A.J., Powers, E.L. Eds, Academic Press, 1981.
19. Sawyer, D.T.; Valentine, J.S. Account. Chem. Res. **1981**, *14*, 393.

MARCEL DEKKER, INC.
270 Madison Avenue, New York, New York 10016

20. Jonsson, M.; Lind, J.; Reitberger, T.; Eriksen, T.E.; Merényi, G. J. Phys. Chem. **1993**, *97*, 8229.
21. Starnes, W.H., Jr. *Symposium on Mechanisms of Autoxidation in Neutral or Alkaline Media*, Raleigh, May 27–29, 1975. Uni Publishers Co., Ltd., 3, 1980.
22. Jonsson, M. J. Phys. Chem. **1996**, *100*, 6814.
23. Ragnar, M.; Lindgren, C.T.; Nilvebrant, N.-O. J. Wood Chem. Techn. **2000**, *20*, 277.
24. Yang, E. *Diss. Royal Inst. of Techn.*, Dept. of Pulp and Paper Chem. and Techn., 1998.
25. *Handbook of Chemistry and Physics 60 ed.*, CRC Press, 1980.
26. Gierer, J.; Nilvebrant, N.-O. Holzforschung **1986**, *40*, 107.
27. Bielski, B.H.J.; Cabelli, D.E.; Arudi, R.L.; Ross, A.B. J. Phys. Chem. Ref. Data **1985**, *14*, 1041.
28. Chuaqui, C.A.; Petkau, A. Radiat. Phys. Chem. **1987**, *30*, 365.
29. Brod, A.J.; Parsons, R.; Jordan, J.J. Eds. *IUPAC Standard Potentials in Aqueous Solution*, Dekker, 1985.
30. Jonsson, M.; Lind, J.; Reitberger, T.; Eriksen, T.E.; Merényi, G. J. Phys. Chem. **1993**, *97*, 8229.
31. Sjögren, B.; Danielsson, J.; Engstrand, P.; Gellerstedt, G.; Zachrisson, H.; Reitberger T. *5th Int. Symp. on Wood and Pulping Chem. Proc.* 161, 1989.
32. Moro-oka, Y.; Foote, C.S. J. Am. Soc. **1976**, *98*, 1510.
33. Lee-Ruff, E. Chem. Soc. Ref. **1977**, 6.
34. Westermark, U. Wood Sci. Techn. **1998**, *16*, 71.
35. Gierer, J.; Imsgard, F. Acta Chem. Scand. **1977**, *B31*, 537.
36. Steenken, S. J. Chem. Soc., Faraday Trans. I. **1987**, *83*, 113.
37. Reitberger, T.; Gierer, J.; Jansbo, K.; Yang, E.; Yoon, B.-H. *6th Int. Symp. on Wood and Pulping Chem. Proc.* Vol. I, 1991.
38. Buxton, G.V. J. Phys. Chem. Ref. Data. **1988**, *17*, 513.
39. Ek, M.; Gierer, J.; Jansbo, K.; Reitberger, T. Holzforschung **1989**, *43*, 391.
40. Lind, J.; Merényi, G.; Nilvebrant, N.-O. J. Wood Chem. Techn. **1997**, *17*, 111.
41. Walling, C. Acc. Chem. Res. **1972**, *8*, 125.
42. Weinstein, J.; Bielski, B.H.J. J. Am. Chem. Soc. **1979**, *101*, 58.
43. Lindén, J.; Öhman, L.-O. Journal of Pulp and Paper Science **1997**, *23*, 193.
44. Lindén, J.; Öhman, L.-O. Journal of Pulp and Paper Science **1998**, *24*, 269.
45. Yasumoto, M.; Matsumoto, Y.; Ishizu, A. J. Wood Chem. Techn. **1996**, *16* (1), 95.

46. Ericsson, B.; Lindgren, B.O.; Theander, O. Cellulose Chem. and Technol. **1973**, *7*, 581.
47. Yokoyama, T. J. Wood Chem. Technol. **1999**, *19*, 187.
48. Landucci, L.L.; Sanyer, N. Tappi. **1975**, *58* (2), 60.
49. Landucci, L-L. Can. Pulp Pap. Assoc. Trans. Tech. Sect. **1978**, *4* (*1*), 25.
50. Stumm W.; Morgan, J.J. *Aquatic Chemistry*, John Wiley and Sons Inc., 1996.

MARCEL DEKKER, INC.
270 Madison Avenue, New York, New York 10016

Request Permission or Order Reprints Instantly!